

Synthesis, Characterization, Molecular Docking and Cytotoxicity Evaluation of New Thienyl Chalcone Derivatives against Breast Cancer Cells

Mohammad Murwih Alidmat¹, Melati Khairuddean¹, Nik Nur Syazni Nik Mohammad Kamal², Musthahimah Muhammad², Habibah A. Wahab³, Mohammad G. Althiabat³, Maram B. Alhwarri³

¹Department of Chemical Sciences, Universiti Sains Malaysia, Penang, Malaysia

²Department of Medical and Dental Sciences, Universiti Sains Malaysia, Penang, Malaysia

³Department of Pharmaceutical Sciences, Universiti Sains Malaysia, Penang, Malaysia

Article History:

Submitted: 15.12.2021

Accepted: 29.12.2021

Published: 05.01.2022

ABSTRACT

Breast cancer is women's most prevalent cancer type. The development of chemotherapy drug resistance and adverse effects is a significant barrier to breast cancer treatment. Recently, the focus of drug discovery has increased toward a valuable structure known as chalcones due to their extensive bioactivity in cancer treatment. In this study, 11 new thienyl chalcone derivatives have been synthesized at room temperature. All the synthesized thienyl chalcone derivatives have been characterized using ATR-FTIR, NMR (1D and 2D). The cytotoxicity activity of all these chalcone compounds was investigated against breast cancer cell lines (MCF-7 and MD-MB-231) and normal breast cell lines (MCF-

10A). The results showed that compounds 5 and 8 exhibited significant cytotoxic activity effects against MCF-7 with IC_{50} $7.79 \pm 0.81 \mu\text{M}$ and $7.24 \pm 2.10 \mu\text{M}$, respectively while the effect against MDA-MB-231 showed the IC_{50} of $5.27 \pm 0.98 \mu\text{M}$ and $21.58 \pm 1.50 \mu\text{M}$, respectively.

Keywords: Chalcone, Thiophene, ER α , Molecular docking, Cytotoxic activity

***Correspondence:** Melati Khairuddean, Department of Chemical Sciences, Universiti Sains Malaysia, Penang, Malaysia, E-mail: melati@usm.my

INTRODUCTION

The prevalence of cancer is increasing worldwide, making it the most leading cause of death in economically developed countries and the second leading cause of death in developing countries (Bray F, *et al.*, 2018). Thus, the need for new chemical entities that selectively combat cancer cells and regulate this disease has continuously risen worldwide (Zhang Z, *et al.*, 2020; Senapati S, *et al.*, 2018). Among the currently identified antitumor agents, chalcones represent an essential class of abundant molecules in edible plants (Singh M, *et al.*, 2020; Banoth RK and Thatikonda A, 2020). Chalcones or α , β -unsaturated carbonyl derivatives are the primary precursor to the biosynthesis of flavonoids and isoflavonoid compounds (Kumar S and Pandey AK, 2013). The chalcones' chemical scaffold consists of two benzene rings separated by a high electrophilic α , β -unsaturated carbonyl system, which give them the semi-planar structure (Amslinger S, 2010). Many of these molecules exhibit beneficial biological activities, including antiprotozoal (García E, *et al.*, 2018), antifungal (Gupta D and Jain DK, 2015), anti-inflammatory (Prabhudeva MG, *et al.*, 2017), antileishmanial (Insuasty B, *et al.*, 2015), antioxidant (Lahsasni SA, *et al.*, 2014; Sökmen M and Khan MA, 2016), antibacterial (Shaik A, *et al.*, 2020), and anticancer activities (Abu N, *et al.*, 2013; Karthikeyan C, *et al.*, 2015; Xiao J, *et al.*, 2021; Wang G, *et al.*, 2020). Recent studies on the anti-proliferative and tumour-reducing activities of some chalcones have increased the interest in exploring chalcone compounds as anticancer agents (Chetana BP, *et al.*, 2009). Chalcone derivatives can be synthesized by several methods such as Suzuki reaction, Wittig reaction, Friedel-Crafts acylation, Aldol condensation, and Photo-Fries rearrangement (Chetana BP, *et al.*, 2009). However, the most common method used is the Claisen-Schmidt reaction of an aromatic aldehyde with

acetophenones (Chavan BB, *et al.*, 2016; Mathew B, *et al.*, 2016). Different series of thienyl chalcone derivatives have been synthesized and have been reported to exhibit a wide range of bioactivity (Shaik AB, *et al.*, 2020; Lokesh BV, *et al.*, 2017). Such compounds with antitumor properties have prompted us to synthesize a series of new unsaturated carbonyl thiophene derivatives and further investigate the cytotoxic ability of these compounds against various breast cancer cell lines.

Estrogen Receptors (ER α and ER β) are vital regulators of breast cancer development (Saha Roy S and Vadlamudi RK, 2012; Hua H, *et al.*, 2018). ER α -positive breast tumors represent 56% of all breast cancer cases, known as hormonal-dependent type breast cancer (Zhang MH, *et al.*, 2014; Yue W, *et al.*, 2013). Thus anti-estrogen, tamoxifen, is considered the primary treatment for hormonal breast cancer. Tamoxifen blocks the estrogenic signal and binds to the Estrogen Receptors, thereby modifying its activity and inhibiting cancer cell growth. Tamoxifen and its active metabolite 4-hydroxytamoxifen (4-OHT) have cytotoxic activity against MCF-7 breast cancer cells. However, the efficacy of tamoxifen is limited by the presence of potential drug resistance (Chang M, 2012; Yao J, *et al.*, 2020).

One of the current strategies to understand the drug-receptor relationship in modern drug discovery is molecular docking. Molecular docking is a computational method that provides information about the molecular interactions of proteins, nucleic acids, lipids, and ligands. Molecular docking gives the optimized conformation of proteins and ligands and their relative orientation through the minimized binding energy (Meng XY, *et al.*, 2011; Rizvi SM, *et al.*, 2013). In this study, different thienyl chalcone derivatives have been designed, synthesized, and investigated as anti-breast cancer *via in-vitro* and *in-silico* studies (Figure 1).

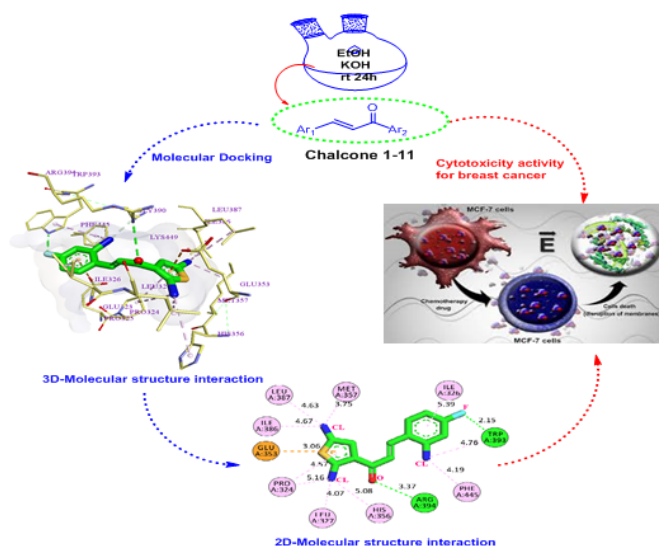


Figure 1: Graphical abstract

MATERIALS AND METHODS

Molecular docking

The X-ray crystal structure of the ER α was downloaded from the RCSB database (PDB ID: 3ERT) (Shiau AK, *et al.*, 1998). Biovia Discovery Studio Visualizer 16.1 was utilized to remove the heteroatoms, water, and prepare the protein further. Eleven synthesized compounds were used as ligands, and tamoxifen was used as a control reference in the docking studies. The 2D chemical structures of all the ligands were built using PerkinElmer ChemDraw software 16.0 and the sketched ligands were then subjected to energy minimization (MM2 force field) using PerkinElmer Chem3D 16.0 and saved in PDB format.

AutoDock 4.2 is a computational software used to prepare the ligands and protein and to generate the docking process (Meng XY, *et al.*, 2011). A click-by-click protocol was used to enforce this process (Rizvi SM, *et al.*, 2013). Initially, the polar hydrogens and Kollman charges were added to the ER α . Then, the selected ligands were revitalized by Gasteiger charges. The grid box's size was set to $50 \times 50 \times 50$, and the coordinates were 31.6615, -0.8435, 25.1743 (as x, y, z, respectively) with a spacing of 0.375. The ER α was defined as rigid for the docking parameter while all ligands were flexible. The genetics algorithm run was set to 100, and the Lamarckian genetic was selected to proceed with the docking, while the remaining parameters were kept as default. Docking scores were interpreted using Discovery Studio Visualizer 16.1 and LigandScout 4.3 academic license, so that the ionic bonds, hydrogen bonds, and hydrophobic interactions could be easily observed (Forli S, *et al.*, 2016).

General method for syntheses of compounds 1-11

The preparation of compounds 1-11 is outlined in Scheme 1-3 using the general preparation method (Ibrahim M, *et al.*, 2012; Ibrahim MM, 2015; Ibrahim MM, *et al.*, 2016). A solution of ketone such as 2-acetylthiophene, 2-acetyl-5-chlorothiophene or 3-acetyl-2,5-dichlorothiophene (0.01 mole) in 25 mL ethanol was added dropwise to a solution containing a selected aldehyde (0.01 mole) and sodium hydroxide (0.02 mol, 2 equiv.) in 5 mL ethanol. The reaction mixture was stirred for 6-24 hours at room temperature. The reaction progress was monitored using TLC. The precipitate formed was filtered off, washed with cold methanol, and dried. The solid product was recrystallized from ethanol (Figures 2-4).

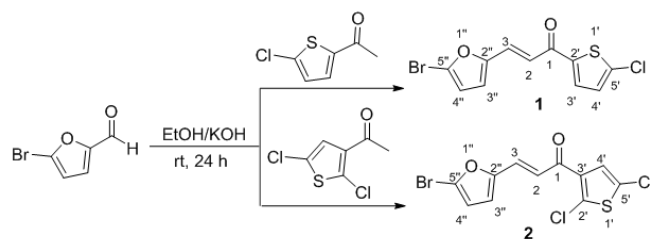


Figure 2: Synthesis of chalcone compounds 1-2

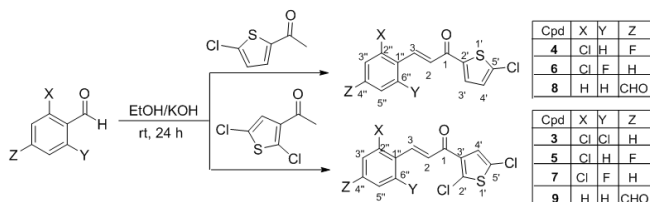


Figure 3: Synthesis of chalcone compounds 3-9

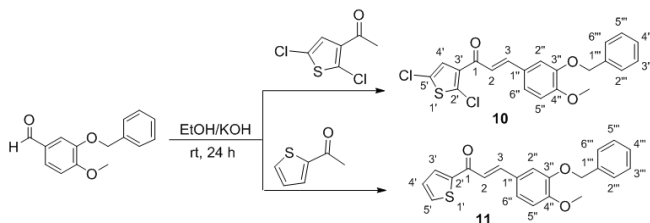


Figure 4: Synthesis of chalcone compounds 10-11

(E)-3-(5''-bromofuran-2''-yl)-1-(5'-chlorothiophen-2'-yl) prop-2-en-1-one, 1

Yield: 85%. Color: yellow solid; mp: 250-252°C. MW: 317.59. IR (cm^{-1}): 3103 ($\text{C}_{\text{sp}^2}\text{-H}$ str.), 1641 (C=O str.), 1588 (C=C aromatic str.), 1529 (C=C alkenyl str.), 778 (C-Cl), 693 (C-Br). $^1\text{H-NMR}$ (500 MHz, CDCl_3) δ , ppm: 7.66 (1H, d, J=4 Hz, H-4''); 7.48 (1H, d, J=15.5 Hz, H-2); 7.21 (1H, d, J=15 Hz, H-3); 7.02 (1H, d, J=4 Hz, H-3''); 6.72 (1H, d, J=3 Hz, H-4''); 6.33 (1H, d, J=3.5 Hz, H-3'''). $^{13}\text{C NMR}$ (125 MHz, CDCl_3) δ , ppm: 114.7 (C-3''), 118.1 (C-3), 118.7 (C-4''), 128.1 (C-5'), 127.7 (C-3'), 128.9 (C-2), 131.3 (C-4'), 139.9 (C-2'), 144.2 (C-5''), 153.2 (C-2''), 180.5 (C-1). CHN Elemental analysis for $\text{C}_{11}\text{H}_6\text{BrClO}_2\text{S}$: Calculated: C, 41.60%; H, 1.90%. Found: C, 41.25%; H, 1.70%.

(E)-3-(5''-bromofuran-2''-yl)-1-(2',5'-dichlorothiophen-3'-yl) prop-2-en-1-one, 2

Yield: 87%. Color: yellow solid; mp: 265-267°C. MW: 352.05. IR (cm^{-1}): 3067 ($\text{C}_{\text{sp}^2}\text{-H}$ str.), 1664 (C=O str.), 1605 (C=C aromatic str.), 1582 (C=C alkenyl str.), 713 (C-Cl), 640 (C-Br). $^1\text{H-NMR}$ (500 MHz, CDCl_3) δ , ppm: 7.69 (1H, s, H-4''); 7.44 (1H, d, J=15.5 Hz, H-2); 7.17 (1H, d, J=16.0 Hz, H-3); 7.15 (1H, d, J=4.25 Hz, H-4''); 6.83 (1H, d, J=15.5 Hz, H-3''). $^{13}\text{C NMR}$ (125 MHz, CDCl_3) δ , ppm: 182.9 (C-1), 153.3 (C-2''), 131.2 (C-2'), 130.5 (C-4''), 128.3 (C-2), 126.9 (C-3'), 126.2 (C-5'), 121.5 (C-4'), 120.7 (C-3), 115.9 (C-3''). CHN Elemental analysis for $\text{C}_{11}\text{H}_5\text{BrCl}_2\text{O}_2\text{S}$: Calculated: C, 37.53%; H, 1.43%; Found: C, 37.84%; H, 1.23%.

(E)-3-(2'',6''-dichlorophenyl)-1-(2',5'-dichlorothiophen-3'-yl) prop-2-en-1-one, 3

Yield: 71%. Color: white solid; mp: 141-143°C. MW: 352.06. IR (cm^{-1}): 3395 ($\text{C}_{\text{sp}^2}\text{-H}$ str.); 1645 (C=O str.); 1583 (C=C str.); 793 (C-Cl); 768 (C-S). $^1\text{H-NMR}$ (500 MHz, CDCl_3) δ , ppm: 7.89 (1H, d, J=16.0 Hz, H-3); 7.40

(1H, d, J=16.0 Hz, H-2), 7.40 (2H, d, J=8.0 Hz, H-3⁵), 7.24 (1H, s, H-4¹), 7.23 (1H, t, J=8.0 Hz, H-4¹). ¹³C NMR (125 MHz, CDCl₃) δ, ppm: 183.3 (C-1), 138.5 (C-3), 137.2 (C-2¹), 135.3 (C-3⁵), 132.2 (C-2⁶), 132.0 (C-1¹), 131.2 (C-4¹), 130.1 (C-4¹), 128.0 (C-3¹), 127.2 (C-2), 127.1 (C-5¹). CHN Elemental analysis for C₁₃H₆Cl₄O₅ Calculated: C, 44.35%; H, 1.72%; Found: C, 44.71%; H, 1.54%.

(E)-3-(2¹-chloro-4¹-fluorophenyl)-1-(5¹-chlorothiophen-2¹-yl)prop-2-en-1-one, 4

Yield: 78%. Color: white solid; mp: 160-162°C. MW: 301.16. IR (cm⁻¹): 3114 (C_{sp}²-H str.); 1650 (C=O str.), 1591 (C=C aromatic str.), 1562 (C=C alkenyl str.), 975 (C-F), 772 (C-Cl). ¹H-NMR (500 MHz, CDCl₃) δ, ppm: 8.15 (1H, d, J=18.0 Hz, H-2), 7.74 (1H, dd, J=7.5 Hz, 8.5 Hz, H-6¹); 7.65 (1H, d, J=4.0 Hz, H-4¹), 7.25 (1H, d, J=16.0 Hz, H-3), 7.22 (1H, d, J=8.5 Hz, H-3¹), 7.07 (1H, ddd, J=2.5 Hz, 8.0 Hz, 10.5 Hz, H-5¹), 7.03 (1H, d, J=4.0 Hz, H-3¹). ¹³C NMR (125 MHz, CDCl₃) δ, ppm: 180.7 (C-1), 164.4 (C-4¹), 143.8 (C-2¹), 140.2 (C-1¹), 139.1 (C-6¹), 136.6 (C-5¹), 131.5 (C-4¹), 129.2 (C-2¹), 127.8 (C-3), 122.7 (C-3¹), 122.7 (C-3¹), 117.8 (C-5¹), 114.9 (C-2). CHN Elemental analysis for C₁₃H₇Cl₂FOS: Calculated: C, 51.85%; H, 2.34%; Found: C, 51.70%; H, 2.54%.

(E)-3-(2¹-chloro-4¹-fluorophenyl)-1-(2,5¹-dichlorothiophen-3¹-yl)prop-2-en-1-one, 5

Yield: 76%. Color: white solid; mp: 132-134°C. MW: 335.62. IR (cm⁻¹): 3064 (C_{sp}²-H str.); 2837 (Csp³-H str.), 1650 (C=O str.), 1588 (C=C aromatic str.), 1568 (C=C alkenyl str.), 811 (C-F), 765 (C-Cl). ¹H-NMR (500 MHz, CDCl₃) δ, ppm: 8.10 (1H, d, J=15.5 Hz, H-2), 7.73 (1H, d, J=9.0 Hz, H-6¹); 7.33 (1H, d, J=15.5 Hz, H-3), 7.28 (1H, s, H-4¹), 7.22 (1H, dd, J=7.3 Hz, 9.0 Hz, H-3¹), 7.07 (1H, ddd, J=2.5 Hz, 8.5 Hz, 16.5 Hz, H-5¹). ¹³C NMR (125 MHz, CDCl₃) δ, ppm: 185.4 (C-1), 164.5 (C-4¹), 139.5 (C-2¹), 137.5 (C-1¹), 136.7 (C-6¹), 131.5 (C-5¹), 129.2 (C-4¹), 127.1 (C-2¹), 125.6 (C-3), 117.8 (C-3¹), 117.6 (C-3¹), 115.02 (C-5¹), 114.8 (C-2). CHN Elemental analysis for C₁₃H₆Cl₃FOS: Calculated: C, 46.52%; H, 1.80%; Found: C, 46.71%; H, 1.74%.

(E)-3-(2¹-chloro-6¹-fluorophenyl)-1-(5¹-chlorothiophen-2¹-yl)prop-2-en-1-one, 6

Yield: 89%. Color: white solid; mp: 144-146°C. MW: 301.16. IR (cm⁻¹): 3106 (C_{sp}²-H str.); 1650 (C=O str.), 1598 (C=C aromatic str.), 1575 (C=C alkenyl str.), 916 (C-F), 732 (C-Cl). ¹H-NMR (500 MHz, CDCl₃) δ, ppm: 8.05 (1H, d, J=16.0 Hz, H-2), 7.65 (1H, d, J=4.0 Hz, H-4¹), 7.62 (1H, d, J=16.0 Hz, H-3), 7.32-7.35 (2H, m, H-3⁴), 7.10 (1H, ddd, J=2.5 Hz, 7.0 Hz, 15.5 Hz, H-5¹), 7.03 (1H, d, J=4.0 Hz, H-3¹). ¹³C NMR (125 MHz, CDCl₃) δ, ppm: 181.2 (C-1), 161.1 (C-6¹), 144.0 (C-1¹), 136.7 (C-5¹), 134.2 (C-4¹), 131.7 (C-3), 131.0 (C-2¹), 127.8 (C-3¹), 127.0 (C-3¹), 126.2 (C-5¹), 121.8 (C-2¹), 115.0 (C-2). CHN Elemental analysis for C₁₃H₇Cl₂FOS: Calculated: C, 51.85%; H, 2.34%; Found: C, 51.71%; H, 2.44%.

(E)-3-(2¹-chloro-6¹-fluorophenyl)-1-(2,5¹-dichlorothiophen-3¹-yl)prop-2-en-1-one, 7

Yield: 69%. Color: white solid; mp: 135-137°C. MW: 335.62. IR (cm⁻¹): 3109 (C_{sp}²-H str.), 1657 (C=O str.), 1591 (C=C aromatic str.), 1565 (C=C alkenyl str.), 883 (C-F), 742 (C-Cl). ¹H-NMR (500 MHz, CDCl₃) δ, ppm: 8.00 (1H, d, J=16.0 Hz, H-3), 7.71 (1H, d, J=16.0 Hz, H-2), 7.31-7.70 (2H, m, H-3⁵), 7.24 (1H, s, H-4¹), 7.10 (1H, ddd, J=2.0 Hz, 7.0 Hz, 15.5 Hz, H-5¹), ¹³C NMR (125 MHz, CDCl₃) δ, ppm: 183.7 (C-1), 163.2 (C-6¹), 137.4 (C-1¹), 136.8 (C-5¹), 135.0 (C-4¹), 132.1 (C-2¹), 131.1 (C-3), 129.7 (C-3¹), 127.1 (C-5¹), 127.0 (C-3¹), 126.2 (C-4¹), 121.8 (C-2¹), 115.0 (C-2). CHN Elemental analysis for C₁₃H₆Cl₃FOS: Calculated: C, 46.52%; H, 1.80%; Found: C, 46.71%; H, 1.94%.

(E)-4-(3-(5¹-chlorothiophen-2¹-yl)-3¹-oxoprop-1¹-en-1¹-yl) benzaldehyde, 8

Yield: 82%. Color: yellow solid; mp: 260-262°C. MW: 276.74. IR (cm⁻¹):

3073 (C_{sp}²-H str.); 1647 (C=O str.), 1588 (C=C aromatic str.), 1526 (C=C alkenyl str.), 719 (C-Cl). ¹H-NMR (500 MHz, CDCl₃) δ, ppm: 10.06 (1H, s, H-1¹); 7.95 (2H, d, J=8.25 Hz, H-2,6); 7.86 (1H, d, J=15.5 Hz, H-1¹); 7.79 (2H, d, J=8.25 Hz, H-3,5); 7.69 (1H, d, J=4.0 Hz, H-3¹); 7.43 (1H, d, J=15.5 Hz, H-2¹); 7.05 (1H, d, J=4.0 Hz, H-4¹). ¹³C NMR (125 MHz, CDCl₃) δ, ppm: 191.4 (C-1¹), 180.5 (C-3¹), 143.8 (C-2¹), 142.5 (C-1¹), 140.5 (C-4), 140.1 (C-5¹), 137.4 (C-1), 131.6 (C-3¹), 130.2 (C-3,5), 129.8 (C-4¹), 129.0 (C-2,6), 123.1 (C-2¹). CHN Elemental analysis for C₁₄H₉ClO₂S: Calculated: C, 60.76%; H, 3.28%; Found: C, 60.71%; H, 3.34%.

(E)-4-(3-(2¹,5¹-dichlorothiophen-3¹-yl)-3¹-oxoprop-1¹-en-1¹-yl) benzaldehyde, 9

Yield: 86%. Color: yellow solid; mp: 173-175°C. MW: 311.19. IR (cm⁻¹): 3326 (C_{sp}²-H str.); 2837 (Csp³-H str.), 1596 and 1516 (C=O str.), 1454 (C=C aromatic str.), 1418 (C=C alkenyl str.), 749 (C-Cl). ¹H-NMR (500 MHz, CDCl₃) δ, ppm: 10.06 (1H, s, H-1¹); 7.95 (2H, d, J=8.25 Hz, H-2,6); 7.86 (1H, d, J=15.5 Hz, H-1¹), 7.79 (2H, d, J=8.25 Hz, H-3,5), 7.43 (1H, d, J=15.5 Hz, H-2¹), 7.22 (1H, s, H-4¹), 7.92 (1H, d, J=8.2 Hz, Ar-C-H=). ¹³C NMR (125 MHz, CDCl₃) δ, ppm: 193.1 (C-1¹), 183.5 (C-3¹), 143.9 (C-1¹), 139.7 (C-4), 136.8 (C-2¹), 130.2 (C-1), 129.1 (C-2, 6), 129.0 (C-3,5), 127.2 (C-4¹), 127.1 (C-5¹), 126.2 (C-3¹), 124.7 (C-2¹). CHN Elemental analysis for C₁₄H₈Cl₂O₂S: Calculated: C, 54.04%; H, 2.59%; Found: C, 53.91%; H, 2.49%.

(E)-3-(3-(benzyloxy)-4-methoxyphenyl)-1-(2,5-dichlorothiophen-3-yl)prop-2-en-1-one, 10

Yield: 83%. Color: yellow solid; mp: 175-177°C. MW: 419.32. IR (v, cm⁻¹): 3102 and 3028 (C_{sp}²-H str.); 2923 and 2833 (Csp³-H str.), 1643 (C=O str.), 1571 (C=C aromatic str.), 1506 (C=C alkenyl str.), 1137 (C-O), 1007 (C-S), 812 (C-Cl). ¹H-NMR (500 MHz, CDCl₃) δ, ppm: 3.96 (s, CH₃, 3H), 5.23 (s, CH₂, 2H), 6.93 (d, J=10.0 Hz, H-2, 1H), 7.12-7.49 (m, H-aromatic, 9H), 7.65 (d, J=15.5 Hz, H-3, 1H). ¹³C-NMR (125 MHz, CDCl₃) δ, ppm: 56.0 (CH₃), 71.2 (CH₂), 111.5 (C-5¹), 112.9 (C-2¹), 121.5 (C-2), 124.0 (C-6¹), 126.8 (C-3¹), 127.2 (C-5¹), 127.2 (C-4¹), 127.3 (C-1¹), 128.1 (C-2¹,6¹), 128.7 (C-4¹), 130.7 (C-3¹,5¹), 136.7 (C-1¹), 138.0 (C-2¹), 145.5 (C-3), 148.3 (C-4¹), 152.4 (C-3¹), 183.8 (C-1). CHN Elemental analysis for C₂₁H₁₆Cl₂O₃S: Calculated: C, 60.15%; H, 3.85%; Found: C, 59.80%; H, 3.49%.

(E)-3-(3-(benzyloxy)-4-methoxyphenyl)-1-(thiophen-2-yl)prop-2-en-1-one, 11

Yield: 78%. Color: yellow solid; mp: 170-173°C. MW: 350.43. IR (v, cm⁻¹): 3022 (C_{sp}²-H str.), 2876 and 2845 (Csp³-H str.), 1649 (C=O str.), 1581 (C=C aromatic str.), 1512 (C=C alkenyl str.), 1134 (C-O), 1010 (C-S). ¹H-NMR (500 MHz, CDCl₃) δ, ppm: 3.95 (s, CH₃, 3H), 5.23 (s, CH₂, 2H), 6.94 (d, J=8.0 Hz, H-2, 1H), 7.19-7.85 (m, H-aromatic, 11H), 7.77 (d, J=15.5 Hz, H-3, 1H). ¹³C NMR (125 MHz, CDCl₃) δ, ppm: 56.0 (CH₃), 71.3 (CH₂), 111.6 (C-5¹), 113.2 (C-2¹), 119.5 (C-6¹), 123.2 (C-2), 127.43 (C-4¹), 127.6 (C-1¹), 128.1 (C-2¹,6¹), 128.1 (C-3¹,5¹), 131.5 (C-3¹), 133.6 (C-5¹), 136.7 (C-1¹), 144.1 (C-2¹), 145.7 (C-3), 148.3 (C-4¹), 152.1 (C-3¹), 182.0 (C-1). CHN Elemental analysis for C₂₁H₁₈O₃S: Calculated: C, 71.98%; H, 5.18%; Found: C, 71.77%; H, 5.39%.

Cell cultures and treatments

The MCF-7, MDA-MB-231, and MCF-10A cells were purchased from the American Type Culture Collection (ATCC, USA). MCF-7 cells were cultured in Roswell Park Memorial Institute-1640 (RPMI-1640) medium with 10% fetal bovine serum (FBS) and 1% penicillin/streptomycin. MDA-MB-231 was cultured in Dulbecco's Modified Eagle Medium (DMEM) medium with high glucose, 10% fetal bovine serum (FBS), and 1% penicillin/streptomycin. The MCF-10A cells were cultured in DMEM/F12 with phenol red solution supplemented with 5% horse serum, 10 µg/mL human insulin, 20 ng/mL hEGF enzyme, 0.5 µg/mL hydrocortisone, and 1% penicillin/streptomycin. Samples (AL1-AL18) were dissolved in Dimethyl Sulphoxide (DMSO) at a stock concentration of 10000 µg/mL and kept at -20°C until use. A stock solution of 10 mM of tamoxifen (Nacalai Tesque,

Japan) was prepared in ethanol, and cisplatin (5 mg/mL, 1.67 mM) with the purity of $\geq 98.0\%$ (T) (Merck, Germany) was prepared in 0.9% sodium chloride, then stored at -20°C until use (Figure 1) (Chuen CS, Pihie AH, 2004).

MTT assay (3-(4,5-Dimethylthiazol-2-yl)-2,5-diphenyltetrazolium Bromide)

In the present study, the MTT cell proliferation assay (Merck Millipore, Germany) cell was used to determine the anti-proliferative effect of 1-11 against MCF-7, MDA-MB-23, and MCF-10A. All cells were seeded in 96-well plates with densities of 1×10^4 cells/well, and left to grow and adhere overnight. The cells were treated with a series of concentrations of 1-11 (0-100 $\mu\text{g}/\text{mL}$), using the cell culture medium as a negative control. In contrast, tamoxifen and cisplatin were used as a positive control. For this analysis, all cells were incubated with respective treatment for 24-72 hours at 37°C in a 5% CO_2 incubator. A standard MTT assay step following Merck Millipore's instructions. Briefly, cells were then labeled with freshly prepared MTT reagent, which has a yellow color. The plates were then incubated at 37°C for 4 hr. The media was removed, and DMSO was added to solubilize the resulting formazan crystals, which have a purple color (Riss TL, *et al.*, 2016). Further analysis was performed using Graph-Pad Prism. The absorbance was recorded using a microplate reader at 570 nm (PowerWave XS, BioTek).

$$\frac{(\text{O.D. treatment}-\text{O.D. blank})/(\text{O.D. untreated cell}-\text{O.D. blank})}{\times 100}$$

(Equation 1)

Assessment on the effect of compounds 1-11 on cell proliferation was repeated thrice independently where all samples, controls, and blanks were prepared in triplicates. The inhibitory concentration of 1-11 to inhibit 50% growth (IC_{50}) was generated from each cell line's dose-response curves.

Selectivity Index (SI)

The degree of selectivity for compounds 1-11 was expressed by its selectivity index (SI), calculated based on Equation 2, which was adapted based on the method reported by Badisa RB, *et al.* (Musa MA, *et al.*, 2010) with minor modification (Badisa RB, *et al.*, 2009).

$$\text{SI} = \text{IC}_{50} \text{ normal cells} / \text{IC}_{50} \text{ cancer cells} \quad (\text{Equation 2})$$

RESULTS AND DISCUSSION

Molecular docking

The behavior of all the 11 thienyl chalcone compounds has been compared with the tamoxifen. To be an effective drug, a compound must have optimum hydrophilic and hydrophobic properties to be transported in blood before penetrating the cell membrane. Water solubility depends on the number of hydrogen bond donors relative to the compound's alkyl side chain. Low water solubility means slow absorption and bioavailability. Too many hydrogen bond donors contribute to low-lipophilicity, leading to the drug's inability to cross the cell membrane. A simple method to evaluate the drug-like properties is to check the compliance with Lipinski's rule (rule of 5), which specifies the numbers of hydrophilic groups, molecular weight, and hydrophobicity. Lipinski's rule of five theorize that an active oral drug should have (i) not more than five hydrogen bond donors (OH and NH groups); (ii) not more than five hydrogen bond acceptors (notably N and O); (iii) molecular weight less than 500 g/mol; and (iv) octanol-water partition coefficient (log P) less than 5 (Zhang MQ, Wilkinson B, 2007). Interestingly, eight out of the 11 thienyl chalcone derivatives complied with Lipinski's rule, as shown in Table 1. Moreover, Table 1 displays the computed scores of docking between the estrogen receptor alpha (ER α) structure (receptor) and all the eleven synthesized compounds (ligands). The more negative value shows a high probability of interaction between the ligand and the receptor. As expected, all the eleven thienyl chalcone derivatives entered the ER α pocket as the tamoxifen and possessed varying scores with the enclosed amino acids.

In Table 1, all the compounds tested showed a good affinity to the active site of ER α with free binding energy ranging from -10.32 to -7.20 kcal/mol. Remarkably, compounds 5 and 8 displayed free binding energy of -10.32 kcal/mol and -10.27 kcal/mol, respectively, which indicated the lowest free binding energy than other derivatives. Both compounds formed a strong interaction in the ER α active site, similar to Tamoxifen. The inhibition constant (K_i) of compounds 5 and 8 was found to be similar with that of Tamoxifen, with the hydrophobic interactions formed with the aromatic rings and the butenyl group. Moreover, a salt bridge interaction (H-bond and ionic bond) was also observed between the tertiary amine and the carboxylic acid group in ASP351, which is considered the most potent form of interaction inside the binding site. Figure 5 shows the docked pose tamoxifen in the binding site of estrogen receptor alpha (ER Th) using Biovia Discovery Studio Visualizer 16.1.

Table 1: Chemical properties based on Lipinski's rule (rule of 5), Free Binding Energy (FBE) with the inhibition constant (K_i) of all 11 thienyl chalcone derivatives, and the tamoxifen (control)

Compound	M.W (g/mol)	Log P	H-bond donor	H-bond acceptor	FBE (Kcal/mol)	Inhibition constant K_i mm (Micromolar)
1	317.59	3.26	0	2	-7.2	5.28
2	352.02	3.58	0	2	-8.01	1.35
3	352.05	5.37	0	1	-8.4	0.693
4	301.16	4.66	0	1	-8.28	0.857
5	335.62	4.97	0	1	-10.32	0.031
6	301.16	4.66	0	1	-7.63	2.56
7	335.62	4.97	0	1	-8.24	0.918
8	276.74	3.69	0	2	-10.27	0.03
9	311.19	4	0	2	-8.29	0.84
10	419.32	5.78	0	3	-9.64	0.085
11	350.43	5.05	0	3	-8.46	0.627
Tamoxifen	371.51	6.07	0	2	-10.4	0.033

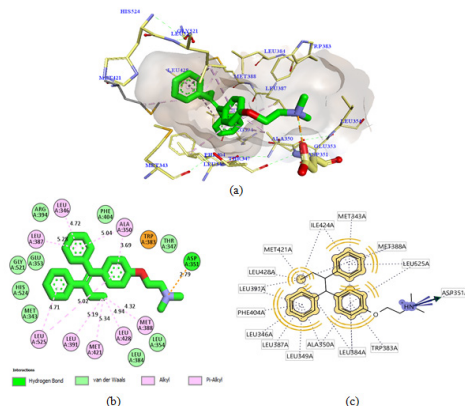


Figure 5: The docked pose of tamoxifen in the binding site of estrogen receptor alpha (ER α): (a) 3D docked interaction, (b) 2D interaction, (c) 2D docked complex using Ligandscore 4.3. The green color represents the carbon atoms in the tamoxifen scaffold, red for oxygen and sky blue for nitrogen atom

Several studies have demonstrated that the biological activity of tamoxifen as an antagonist to ER α was moderate compared to 4-hydroxytamoxifen. The inhibition potential of 4-hydroxy tamoxifen was 30-100 times more efficacious than tamoxifen against breast cancer line MCF-7 (Zhong Q, *et al.*, 2015; Maximov PY, *et al.*, 2018; Molina L, *et al.*, 2020; Fröhlich T, *et al.*, 2020). Consequently, *in silico* studies are important in interpreting the critical amino acid interactions inside the active site of ER α that are liable on the activity. Interaction with ASP351 is responsible for ligand activity, while to be potent, a ligand should form H-bond with the residue ARG394 and/or GLU353 in the active site (Kelly PM, *et al.*, 2017; Luo G, *et al.*, 2017; Shtaiwi A, *et al.*, 2019).

Based on the main interactions between tamoxifen and ER α , a new design of thienyl chalcone derivatives has been launched by adding various halogens in the aromatic rings. The findings have shown that the aromatic ring in compound 5 and 8 formed hydrophobic interactions in the binding site of ER α which were found to be substantially similar to Tamoxifen (Figure 6). The docking results of compound 5 formed the pi-anion bond with GLU353 and another hydrogen bond with TRP393 at a distance of 2.15 Å. Strikingly, the thiol group in compound 8 formed one covalent bond (disulfide bond) with the thiol group of MET42. This improved and stabilized the interaction within the active site for a long time, which is essential and needed to inhibit the activity of ER α . As a result, compounds 5 and 8 exhibited the hydrogen bond interaction with the ARG394 in the ER α active site, which explained their cytotoxic activity *in-vitro* assay.

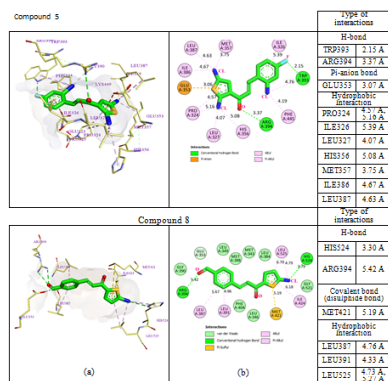


Figure 6: The best predicted binding poses of (a) 2D- and (b) 3D-molecular structure interaction of compounds 5 and 8 with 3ERT.PDB. In the scaffold, green color represents the carbon atoms, red for oxygen, sky blue for fluorine, dark blue for chlorine, and pale blue for the nitrogen atom

Structure confirmation

The synthesis of thienyl chalcone derivatives was accomplished via the Claisen-Schmidt condensation reaction. The proposed mechanism for this reaction is shown in Figure 7. In step (1), deprotonation of α -carbon generates the enolate, which forms the resonance-stabilized structure. The nucleophilic attack of this enolate at the electrophilic carbon of benzaldehyde in step (2), followed by protonation in step (3) forms a β -hydroxy carbonyl. Dehydration of the product through E1CB pathway in step (4) involves the abstraction of the acidic hydrogen at the α -carbon to form a carbanion. The electron on the carbanion moves to form a double bond while cleaving the leaving group (OH) in step [5], which gave a good yield of chalcone.

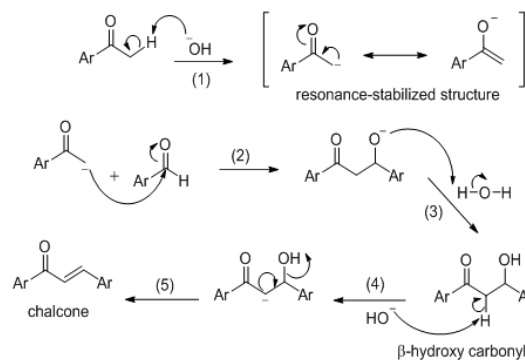


Figure 7: Proposed mechanism of base-catalyzed thienyl chalcones derivatives preparation

Chalcone 1 is used as a representative compound for structure confirmation. The IR spectrum of chalcone 1 (Figure 8) shows one weak absorption band at 3067 cm^{-1} , assigned for the $\text{C}_{\text{sp}^2}\text{-H}$ stretching. The absorption bands at 1664 cm^{-1} and 1582 cm^{-1} for the $\text{C}=\text{O}$ and $\text{C}=\text{C}$ alkenyl, respectively, confirmed the α,β -unsaturated moiety of the chalcone while other bands at 1588 cm^{-1} , 778 cm^{-1} and 693 cm^{-1} were assigned to the $\text{C}=\text{C}$ aromatic, $\text{C}-\text{Cl}$ and $\text{C}-\text{Br}$ stretchings, respectively.

In Figure 9, the ^1H NMR spectrum of chalcone 1 shows six signals including two doublets at δH 7.22 and 7.46 (H-2 and H-3), assigned for the alkenyl protons which indicated the presence of a *trans* geometrical isomer. This was confirmed based on the coupling constant value of $J=15.5$ Hz. Four other signals were ascribed to the aromatic protons, two doublets of the thiophene ring at δH 7.02 and 7.62 (H-3' and H-4'), and two doublets of the furan ring at δH 6.40 and 6.68 (H-3'' and H-4'').

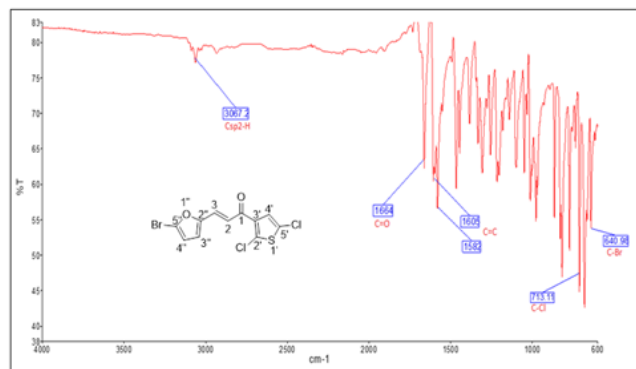


Figure 8: IR spectrum of chalcone 1

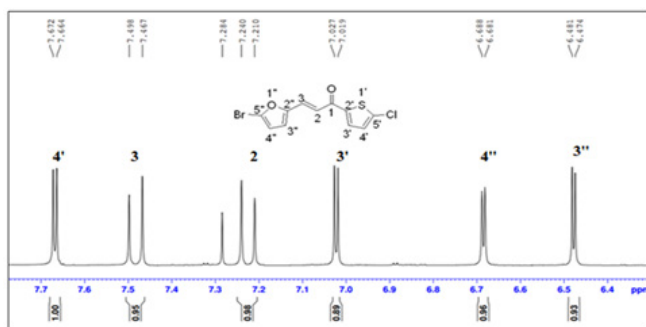


Figure 9: ¹H-NMR spectrum of chalcone 1 (500 MHz, CDCl₃)

In Figure 10, the ¹³C-NMR spectrum of chalcone 1 shows eleven carbon signals. Four carbons for the thiophene ring, C-5'(144.2), C-2'(139.9), C-4'(131.3) and C-3'(127.8), four carbons for the furan ring, C-2''(153.2), C-5''(126.2), C-4''(118.2) and C-3''(114.7)), two carbons for the alkene group, C-2(118.7) and C-3(128.9) and a carbonyl carbon in the most downfield region, C-1(180.5).

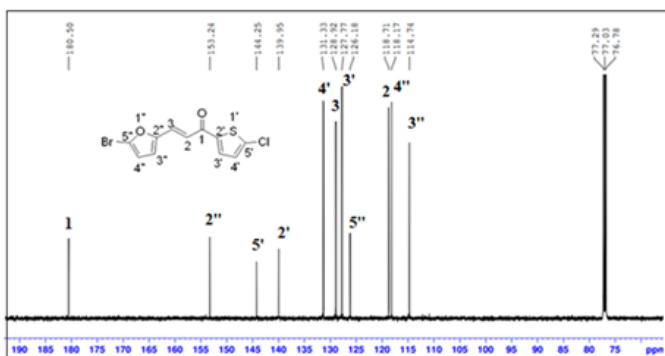


Figure 10: ¹³C-NMR spectrum of chalcone 1 (125 MHz, CDCl₃)

The DEPT experiment differentiates between CH, CH₂ and CH₃ groups by variation of the selection angle parameter. The 45° angle gives all carbons with the attached protons (regardless of number) in the positive phase. So, DEPT-45 shows all the carbons, The 90° angle (DEPT-90) shows only the CH while the others are suppressed. A complete assignment of all carbon signals of mono-chalcone 1 was done using DEPT-90 which showed the methine (CH) carbons as positive signals. In Figure 11, two alkenyl and four aromatic protons appeared as four signals in the positive phase while no carbonyl carbon signal was observed as it is a quaternary carbon.

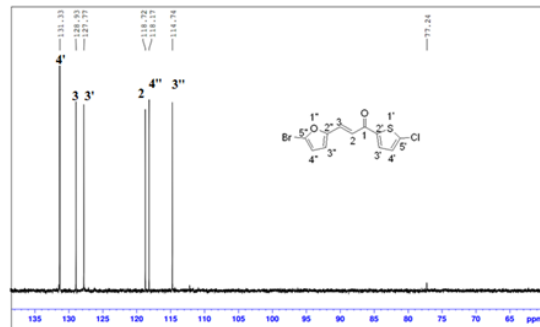


Figure 11: DEPT-90 spectrum of mono-chalcone 1

¹H-¹H Correlation Spectroscopy (COSY) shows the correlation between hydrogens which are coupled to each other in the ¹H NMR spectrum. The ¹H spectrum is plotted on both 2D axes. While 2-bond and 3-bond ¹H-¹H coupling is easily visible by COSY, long-range coupling can also be observed with long acquisition times. The HSQC (Heteronuclear Single Quantum Coherence) experiment is used to determine proton-carbon single bond correlations, where the protons lie along the observed F2 (X) axis and the carbons are along the F1 (Y) axis. The HMBC (Heteronuclear Multiple Bond Correlation) experiment gives correlations between carbons and protons that are separated by two, three, and, sometimes in conjugated systems, four bonds. Direct one-bond correlations are suppressed. This gives connectivity information much like a proton-proton COSY. Figure 12 shows the 2D NMR of 1H-1H COSY correlation in which H-3'' coupled with H-4'', while H-4'' coupled with H-3''. The H-3' coupled with H-4', while H-4' coupled with H-3', while H-2 coupled with H-3, and H-3 coupled with H-2.

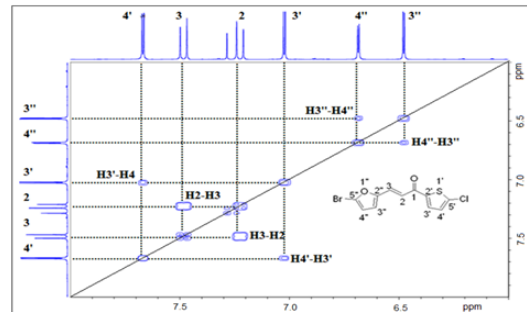


Figure 12: COSY (1H-1H) spectrum of chalcone 1

Figure 13 shows a correlation between carbon and its proton for chalcone 1. The HSQC (Heteronuclear Single Quantum Coherence) experiment provides a direct proton-carbon correlation. Based on the spectrum in Figure 9, the protons at δH 7.62 (H-4'), 7.40 (H-3), 7.22 (H-2), 7.02 (H-3'), 6.68 (H-4'') and 6.40 (H-3'') showed correlations with C-4' (131.3), C-2 (128.9), C-3 (118.2), C-3' (127.8), C-4'' (118.7), and C-3'' (114.7), respectively.

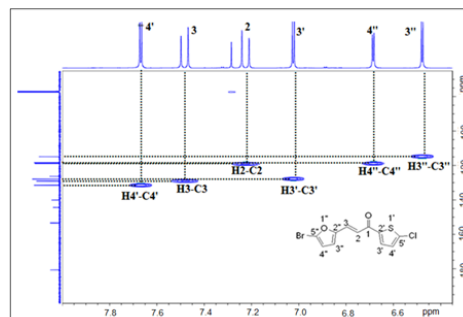


Figure 13: HSQC spectrum (1H-¹³C of a direct coupling) of chalcone 1

Figure 14 of the HMBC ($1H-^{13}C$ of a long-range coupling) showed the cross-peaks between H-4' with C-5'(144.2), C-2'(139.9), and C-2'' (153.2). Several other cross-peaks observed were between H-3 with C-2'' (153.2), and C-1 (180.5). between H-2 with C-2'' (153.2), and C-1 (180.5), between H-3' with C-5'(144.2), between H-4'' with C-3''(114.7), C-5''(126.2), and C-2'' (153.2), and finally between H-3'' with C-5''(126.2), and (C-2'' (153.2). All these coupling data of chalcone 1 are summarised in Table 2.

Cytotoxicity activity

The MTT assay was used to test the cytotoxic activity effect of all the newly synthesized thienyl chalcone derivatives, 1-11, against two breast cancer cell lines (MCF-7 and MDA-MB-231). The cytotoxic activity has also been assessed towards the normal breast cell line (MCF-10A) to evaluate the cytotoxic activity and the selectivity index toward the healthy tissue. The results indicated that some of the synthesized compounds exhibit moderate to potent cytotoxic activity against the tested breast cancer cell lines.

Based on the IC_{50} values of the tested compounds in Figure 15, the MTT assay showed that compounds 5 and 8 were the most active, while the remaining compounds were moderately active to inactive against the cancer cell lines tested. After 48 hours of exposure to compounds 5 and 8, significant inhibition of cancer cell proliferation in the treated cells was observed compared to the control cells. Compound 5 was the most active against the MDA-MB-231 cancer cell line and demonstrated a potent cytotoxic activity with IC_{50} of $6.15 \pm 1.24 \mu M$ while compound 8 was the most active against the MCF-7 cancer cell line with IC_{50} of $7.14 \pm 2.10 \mu M$. The results of cell viability inhibition of 1-11 against different breast cancer cell lines shown in Figure 8 are summarized in Table 3. Most of the tested compounds showed the lowest cell viability at 48 hours of incubation. On the other hand, cell viability increased at 72 hrs. This might be due to the possible propagation of the remaining uninfluenced cells. Furthermore, the improvement of cell viability after 48 hrs exposure suggests the anti-proliferative effect of the tested compounds rather than cytotoxic effect toward breast cancer cell lines.

The MTT assay findings displayed the cytotoxic activity of the synthesized compounds and their selectivity towards cancerous cells. Interestingly, compounds 5 and 8 showed good selectivity toward cancerous cell lines relative to a healthy cell. Compound 8 was found to be 14-fold less active towards normal human breast epithelial cells (MCF-10A) than MCF-7 cells, while, compound 5 was found to be 6-fold less active toward the normal cell (MCF-10A) compared to MDA-MB-231. As a result, compounds 5 and 8 showed better cytotoxic activity with high selectivity toward cancerous cells compared to tamoxifen. Previous studies have reported that the tamoxifen selectivity index of nearly one toward MCF-7 and MDA-MB-231. The promising cytotoxic activity and selectivity of compounds 5 and 8 on MCF-7 and MDA-MB-231 cells encouraged further investigation of the cytotoxic activity through mechanistic cell growth inhibition of cancer cells at the cellular level. The selectivity of all the tested compounds against the healthy cell line is presented in Figure 16.

Based on the Structure-Activity Relationship (SAR) between the synthesized compounds and the results of the cytotoxic assay, the electron-withdrawing group on ring A and ring B is vital for cytotoxic activity (Figure 17). Compounds 1 and 2 with furan ring substitution at carbon β to the carbonyl group demonstrated less cytotoxicity than phenyl substitution. The insertion of the halogen group (chloro) at the para position (5') of the thiophene ring improves the activity only when ring B is phenyl. Further study of SAR has shown that the electron-withdrawing group position on the phenyl ring is essential (Wilcken R, *et al.*, 2013). Compounds 5 and 7 have two halogen atoms on the phenyl ring (chloro and fluoro) but at different positions. This dramatically changes the cytotoxicity results. The influence of chloro substituent was reported to increase the cytotoxic activity of various chalcone compounds (Liew SK, *et al.*, 2020). However, an aldehyde substituent at the para position of the phenyl ring in compound 8 compensates for both fluoro and chloro since this carbonyl group is a more substantial electron-withdrawing group than halogen. Consequently, compounds 5 and 8 showed a significant cytotoxic activity due to the existence of well-established cytotoxic enhancer groups such as; carbonyl, fluoro, and chloro.

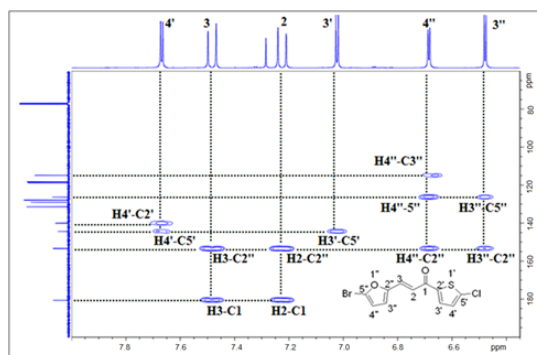


Figure 14: HMBC spectrum ($1H-^{13}C$ of a long-range coupling) of chalcone 1

Table 2: Summary of COSY ($1H-1H$); HSQC ($1H-^{13}C$ of a direct coupling) and HMBC ($1H-^{13}C$ of a long-range coupling) of chalcone 1

1D-NMR				2D-NMR		
Proton	$1H \delta$ (ppm)	C	δ (ppm)	COSY ($1H-1H$)	HSQC ($1H-^{13}C$)	HMBC ($1H-^{13}C$)
H-3''	6.34(d, J=3.5 Hz, 1H)	C-3''	114.7	H-4''	C-3''(114.7)	C-5''(126.2), C-2''(153.2).
		C-3	118.1			
		C-4''	118.7			
		C-5'	128.1			
		C-3'	127.7			
		C-2	128.9			
		C-4'	131.3			

H-4''	6.72(d, J=3 Hz, 1H)	C-2'	139.9	H-3''	C-4''(118.7)	C-3''(114.7), C-5''(126.2),
		C-5''	144.2			C-2''(153.2)
H-3'	7.02 (d, J=4 Hz, 1H)	C-2''	153.2	H-4'	C-3'(127.8)	C-5'(144.2)
H-3	7.21(d, J=15Hz, 1H)	C-1	180.5	H-2	C-3(118.2)	C-2''(153.2), C-1(180.5),
H-2	7.48(d, J=15.5 Hz, 1H)			H-3	C-2(128.9)	C-2''(153.2), C-1(180.5).
H-4'	7.66(d, J=4 Hz, 1H)			H-3'	C-4'(131.3)	C-5'(144.2), C-2'(139.9), C-2''(153.2).

Note: ' -Functional groups; '' -Lower state of quantum number

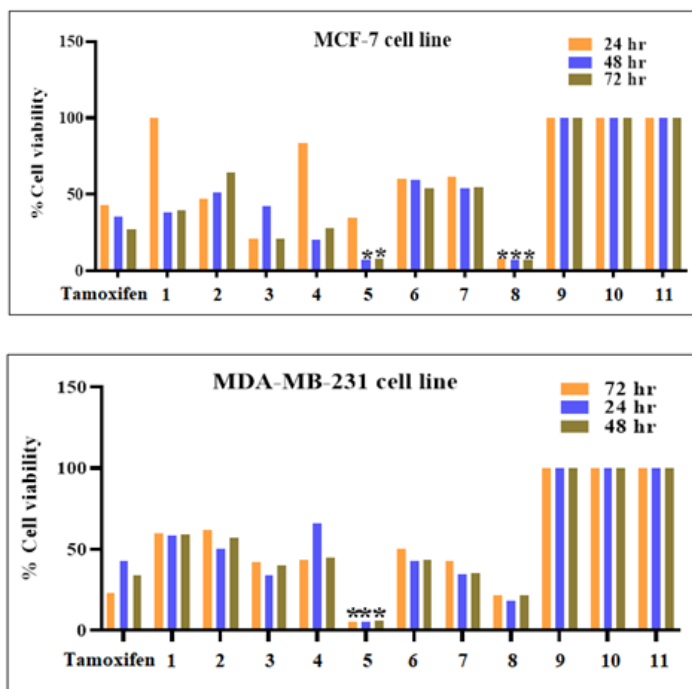
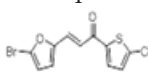
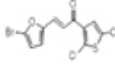
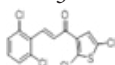
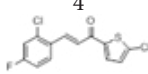
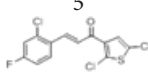
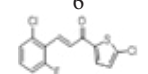
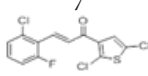
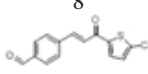
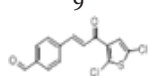
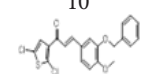
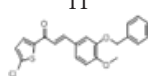
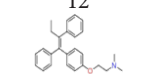


Figure 15: Cytotoxic activity expressed by IC_{50} values of thienyl chalcone derivatives, 1-11 against several cell lines (MCF-7 and MDA-MB-231). * $P < 0.0001$ vs. the control

Table 3: IC_{50} values and selectivity index of thienyl chalcone compounds, 1-11 against several cell lines (MCF-7, MDA-MB-231, and MCF-10A)

Compounds	Time (h)	IC_{50} (μ M)			Selective index (IC_{50} in normal cells/ IC_{50} in cancer cells)	
		MCF-7	MDA-MB-231	MCF-10A	MCF-7	MDA-MB-231
	24	100 \pm 0.01	58.89 \pm 1.36	100 \pm 0.01	1	1.7
	48	38.1 \pm 2.97	59.12 \pm 1.41	100 \pm 0.01	2.62	1.69
	72	39.57 \pm 2.87	60.03 \pm 0.40	100 \pm 0.01	2.53	1.67
	24	47.19 \pm 2.75	50.70 \pm 0.58	100 \pm 0.01	2.12	1.97
	48	50.91 \pm 1.36	57.32 \pm 0.38	100 \pm 0.01	1.99	1.74
	72	64.6 \pm 2.61	62.15 \pm 1.64	100 \pm 0.01	1.55	1.61
	24	83.24 \pm 3.83	33.66 \pm 1.94	79.0 \pm 6.35	0.95	2.35
	48	20.27 \pm 0.54	40.44 \pm 1.08	44.69 \pm 1.80	2.2	1.11
	72	21.24 \pm 1.11	42.33 \pm 0.56	44.0 \pm 1.16	2.07	1.04

	24	100 ± 0.01	66.12 ± 3.04	100 ± 0.01	1	1.51
	48	26.36 ± 2.15	44.68 ± 1.03	100 ± 0.01	3.79	2.24
	72	27.90 ± 1.47	43.87 ± 5.49	100 ± 0.01	3.58	2.28
	24	34.55 ± 3.85	6.15 ± 1.24	44.03 ± 7.32	1.27	7.16
	48	7.24 ± 0.33	6.26 ± 0.08	36.07 ± 2.08	4.98	5.76
	72	7.79 ± 0.81	5.27 ± 0.98	30.7 ± 1.77	3.94	5.83
	24	60.35 ± 0.16	42.68 ± 1.68	74.81 ± 4.87	1.24	1.75
	48	59.35 ± 1.57	43.34 ± 1.52	71.36 ± 1.88	1.2	1.65
	72	54.21 ± 3.77	50.69 ± 5.22	65.58 ± 1.76	1.21	1.29
	24	61.25 ± 3.21	34.87 ± 8.67	100 ± 0.01	1.63	2.87
	48	53.71 ± 1.24	35.72 ± 4.96	100 ± 0.01	1.86	2.8
	72	54.59 ± 3.14	42.95 ± 5.97	100 ± 0.01	1.83	2.33
	24	8.16 ± 0.87	18.22 ± 1.13	87.16 ± 4.01	10.68	4.78
	48	7.14 ± 0.19	21.89 ± 1.01	100 ± 0.01	14	4.57
	72	7.24 ± 2.10	21.58 ± 1.50	100 ± 0.01	13.81	4.63
	24	100 ± 0.01	100 ± 0.01	100 ± 0.01	1	1
	48	100 ± 0.01	100 ± 0.01	100 ± 0.01	1	1
	72	100 ± 0.01	100 ± 0.01	100 ± 0.01	1	1
	24	100 ± 0.01	100 ± 0.01	100 ± 0.01	1	1
	48	100 ± 0.01	100 ± 0.01	100 ± 0.01	1	1
	72	100 ± 0.01	100 ± 0.01	100 ± 0.01	1	1
	24	100 ± 0.01	100 ± 0.01	100 ± 0.01	1	1
	48	100 ± 0.01	100 ± 0.01	100 ± 0.01	1	1
	72	100 ± 0.01	100 ± 0.01	100 ± 0.01	1	1
	24	42.66 ± 2.19	43.03 ± 1.60	-	-	-
	48	35.01 ± 3.28	34.19 ± 3.04	-	-	-
	72	26.95 ± 3.01	23.36 ± 3.84	-	-	-

Note: MCF-7: Michigan Cancer Foundation-7; MDA-MB-231: MD Anderson with Model late-stage Breast cancer

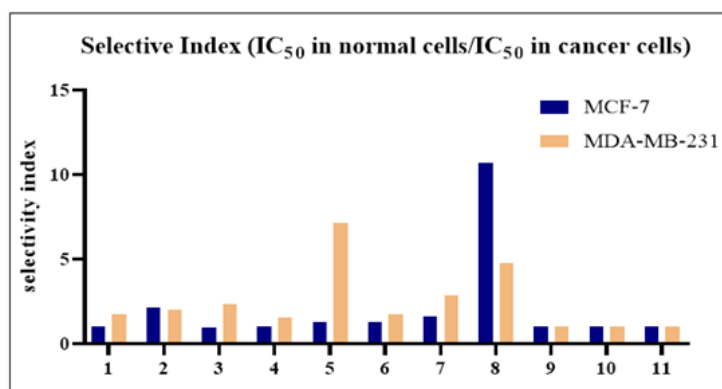


Figure 16: The selectivity index of compounds 1-11, IC_{50} in non-cancerous MCF-10A cell line/ IC_{50} in cancerous cell line (MCF-7, MDA-MB-231)

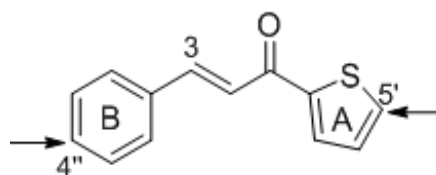


Figure 17: Structure-Activity Relationship of thienyl chalcone derivatives

CONCLUSION

In this study, 11 new thienyl chalcone derivatives were synthesized via the Claisen-Schmidt condensation in basic media. These compounds were characterized by IR and NMR spectroscopic techniques and CHN elemental analysis before being evaluated for their cytotoxicity activity against breast cancer cell lines MCF-7 and MDA-MB-231. The results showed that compound 5 exhibited significant cytotoxic activity with the IC₅₀ values of 7.79 ± 0.81 μM (MCF-7) and 5.27 ± 0.98 μM (MDA-MB-231) while compound 8 displayed the IC₅₀ values of 7.24 ± 2.10 μM (MCF-7) and 21.58 ± 1.50 μM (MDA-MB-231) after 72 hr incubation. It can be concluded that cytotoxicity studies for anticancer are significantly dependent on the number of the substituents attached to the thienyl chalcone scaffold whereby compound with more substituents tends to exhibit better antitumor activities. The presence of electron-withdrawing groups was found to enhance the cytotoxicity to a certain degree. The chloro, fluoro, and carbonyl substituents on the phenyl ring of the synthesized compounds play an important role in cytotoxic enhancement compared to the furan ring.

The molecular docking analysis showed that a compound with a larger structure has an increasing number of bonds, leading to more interactions with the residues of amino acids in the active ER α site, which could have enhanced the antitumor activity. Furthermore, the docking scores showed that the binding energies of the synthesized compounds 5 and 8 to the ER α receptor were the best of all the synthesized derivatives. These findings were broadly compatible with the observed *in vitro* assay investigation. Therefore, further investigation on the molecular modeling and docking studies using AutoDock1.5.6 tools can be used to predict the best structure with the highest affinity to bind to the breast cancer cell line. Various interactions between the designed compounds (ligands) and receptor active sites will be used to design new chalcone derivatives with better functions for anticancer drugs in the future.

DECLARATIONS

Acknowledgement

The authors would like to thank Universiti Sains Malaysia, Penang, Malaysia, and the Malaysian Government for the Fundamental Research Grant Scheme (FRGS) 1/2019 (203.PKIMIA.6711789) which was used to finance this research work.

Availability of data and material

All data generated or analysed during this study are included in this published article and its supplementary information files.

REFERENCES

1. Bray F, Ferlay J, Soerjomataram I, Siegel RL, Torre LA, Jemal A. Global cancer statistics 2018: GLOBOCAN estimates of incidence and mortality worldwide for 36 cancers in 185 countries. *Ca Cancer J Clin.* 2018; 68(6): 394-424.
2. Zhang Z, Zhou L, Xie N, Nice EC, Zhang T, Cui Y, *et al.* Overcoming cancer therapeutic bottleneck by drug repurposing. *Signal Transduct Target Ther.* 2020; 5(1): 1-25.
3. Senapati S, Mahanta AK, Kumar S, Maiti P. Controlled drug delivery vehicles for cancer treatment and their performance. *Signal Transduct Target Ther.* 2018; 3(1): 1-9.
4. Singh M, Sharma P, Joshi P, Saini K, Sharma A, Puri V, *et al.* Chalcones: A privileged scaffold with diverse biological activities. *Plant Arch.* 2020; 20(1): 3812-3819.
5. Banoth RK, Thatikonda A. A review on natural chalcones an update. *Int J Pharm Sci Res.* 2020; 11(2): 546-555.
6. Kumar S, Pandey AK. Chemistry and biological activities of flavonoids: an overview. *Sci World J.* 2013; 2013.
7. Amslinger S. The Tunable functionality of α, β-unsaturated carbonyl compounds enables their differential application in biological systems. *Chem Med Chem.* 2010; 5(3): 351-356.
8. García E, Coa JC, Otero E, Carda M, Vélez ID, Robledo SM, *et al.* Synthesis and antiprotozoal activity of furanchalcone-quinoline, furanchalcone-chromone and furanchalcone-imidazole hybrids. *Med Chem Res.* 2018; 27(2): 497-511.
9. Gupta D, Jain DK. Chalcone derivatives as potential antifungal agents: Synthesis, and antifungal activity. *J Adv Pharm Technol Res.* 2015; 6(3): 114.
10. Prabhudeva MG, Bharath S, Kumar AD, Naveen S, Lokanath NK, Mylarappa BN, *et al.* Design and environmentally benign synthesis of novel thiophene appended pyrazole analogues as anti-inflammatory and radical scavenging agents: Crystallographic, *in silico* modeling, docking and SAR characterization. *Bioorg Chem.* 2017; 73: 109-120.
11. Insuasty B, Ramírez J, Becerra D, Echeverry C, Quiroga J, Abonia R, *et al.* An efficient synthesis of new caffeine-based chalcones, pyrazolines and pyrazolo [3, 4-b] [1, 4] diazepines as potential antimalarial, antitrypanosomal and antileishmanial agents. *Eur J Med Chem.* 2015; 93: 401-413.
12. Lahsasni SA, Al Korbi FH, Aljaber NA. Synthesis, characterization and evaluation of antioxidant activities of some novel chalcones analogues. *Chem Cent J.* 2014; 8(1): 1-10.
13. Sökmen M, Khan MA. The antioxidant activity of some curcuminoids and chalcones. *Inflammopharmacology.* 2016; 24(2): 81-86.
14. Shaik A, Bhandare RR, Palleapati K, Nissankararao S, Kancharlappalli V, Shaik S. Antimicrobial, antioxidant, and anticancer activities of some novel isoxazole ring containing chalcone and dihydropyrazole derivatives. *Molecules.* 2020; 25(5): 1047.
15. Abu N, Akhtar MN, Ho WY, Yeap SK, Alitheen NB. 3-Bromo-1-hydroxy-9, 10-anthraquinone (BHAQ) inhibits growth and migration of the human breast cancer cell lines MCF-7 and MDA-MB231. *Molecules.* 2013; 18(9): 10367-10377.
16. Karthikeyan C, SH Narayana Moorthy N, Ramasamy S, Vanam U, Manivannan E, Karunakaran D, *et al.* Advances in chalcones with anticancer activities. *Recent Pat Anticancer Drug Discov.* 2015; 10(1): 97-115.
17. Xiao J, Gao M, Diao Q, Gao F. Chalcone Derivatives and their Activities against Drug-resistant Cancers: An Overview. *Curr Top Med Chem.* 2021; 21(5): 348-362.
18. Wang G, Liu W, Gong Z, Huang Y, Li Y, Peng Z. Synthesis, biological evaluation, and molecular modelling of new naphthalene-chalcone derivatives as potential anticancer agents on MCF-7 breast cancer cells by targeting tubulin colchicine binding site. *J Enzyme Inhib Med Chem.* 2020; 35(1): 139-144.
19. Chetana BP, Mahajan SK, Suvarna AK. Chalcone: A versatile molecule. *J Pharm Sci Res.* 2009; 1(3): 11-22.
20. Chavan BB, Gadekar AS, Mehta PP, Vawhal PK, Kolsure AK, Chabukswar AR. Synthesis and Medicinal Significance of Chalcones: A Review. *Asian J Biomed Pharm Sci.* 2016; 6(56): 01.
21. Mathew B, Haridas A, Uçar G, Baysal I, Adeniyi AA, Soliman ME, *et al.* Exploration of chlorinated thienyl chalcones: A new class of monoamine oxidase-B inhibitors. *Int J Biol Macromol.* 2016; 91: 680-695.

22. Shaik AB, Bhandare RR, Nissankararao S, Edis Z, Tangirala NR, Shahanaaz S, *et al.* Design, facile synthesis and characterization of dichloro substituted chalcones and dihydropyrazole derivatives for their antifungal, antitubercular and antiproliferative activities. *Molecules*. 2020; 25(14): 3188.
23. Lokesh BV, Prasad YR, Shaik AB. Synthesis and biological activity of novel 2, 5-dichloro-3-acetylthiophene chalcone derivatives. *Ind J Pharm Educ Res*. 2017; 51: 679-690.
24. Saha Roy S, Vadlamudi RK. Role of estrogen receptor signaling in breast cancer metastasis. *Int J Breast Cancer*. 2012; 2012.
25. Hua H, Zhang H, Kong Q, Jiang Y. Mechanisms for estrogen receptor expression in human cancer. *Exp Hematol Oncol*. 2018; 7(1): 1-1.
26. Zhang MH, Man HT, Zhao XD, Dong N, Ma SL. Estrogen receptor-positive breast cancer molecular signatures and therapeutic potentials. *Biomed Rep*. 2014; 2(1): 41-52.
27. Yue W, Yager JD, Wang JP, Jupe ER, Santen RJ. Estrogen receptor-dependent and independent mechanisms of breast cancer carcinogenesis. *Steroids*. 2013; 78(2): 161-170.
28. Chang M. Tamoxifen resistance in breast cancer. *Biomol Ther*. 2012; 20(3): 256.
29. Yao J, Deng K, Huang J, Zeng R, Zuo J. Progress in the understanding of the mechanism of tamoxifen resistance in breast cancer. *Front Pharmacol*. 2020; 11.
30. Meng XY, Zhang HX, Mezei M, Cui M. Molecular docking: A powerful approach for structure-based drug discovery. *Curr Comput Aided Drug Des*. 2011; 7(2): 146-157.
31. Rizvi SM, Shakil S, Haneef M. A simple click by click protocol to perform docking: AutoDock 4.2 made easy for non-bioinformaticians. *EXCLI J*. 2013; 12: 831.
32. Shiau AK, Barstad D, Loria PM, Cheng L, Kushner PJ, Agard DA, *et al.* The structural basis of estrogen receptor/coactivator recognition and the antagonism of this interaction by tamoxifen. *Cell*. 1998; 95(7): 927-937.
33. Forli S, Huey R, Pique ME, Sanner MF, Goodsell DS, Olson AJ. Computational protein-ligand docking and virtual drug screening with the AutoDock suite. *Nat Protoc*. 2016; 11(5): 905-919.
34. Ibrahima M, Al-Refaia M, El-Halawaa R, Tashtousha H, Alsohailib S, Masadc M. Synthesis of some new chalcone and 4, 5-Dihydro-1H-PyrazoleDerivatives as potential antimicrobial agents. *Jor J Chem*. 2012; 7(2): 115-123.
35. Ibrahim MM. Synthesis and characterization of new 3, 5-disubstituted-4, 5-dihydro-1H-pyrazole and their carbothioamide derivatives. *Eur J Chem*. 2015; 6(1): 78-83.
36. Ibrahim MM, Al-Refai M, Ayub K, Ali BF. Synthesis, spectral characterization and fluorescent assessment of 1, 3, 5-Triaryl-2-pyrazoline derivatives: Experimental and theoretical studies. *J Fluoresc*. 2016; 26(4): 1447-1455.
37. Chuen CS, Pihie AH. Eurycomanone exerts antiproliferative activity via apoptosis upon MCF-7 cells. *Proceedings of the 4th Annual Seminar of National Science Fellowship*. 2004.
38. Riss TL, Moravec RA, Niles AL, Duellman S, Benink HA, Worzella TJ, *et al.* Cell viability assays. *Assay Guidance Manual*. 2016.
39. Musa MA, Badisa VL, Latinwo LM, Waryoba C, Ugochukwu N. *In vitro* cytotoxicity of benzopyranone derivatives with basic side chain against human lung cell lines. *Anticancer Res*. 2010; 30(11): 4613-4617.
40. Badisa RB, Darling-Reed SF, Joseph P, Cooperwood JS, Latinwo LM, Goodman CB. Selective cytotoxic activities of two novel synthetic drugs on human breast carcinoma MCF-7 cells. *Anticancer Res*. 2009; 29(8): 2993-2996.
41. Zhang MQ, Wilkinson B. Drug discovery beyond the 'rule-of-five'. *Curr Opin Biotechnol*. 2007; 18(6): 478-488.
42. Zhong Q, Zhang C, Zhang Q, Miele L, Zheng S, Wang G. Boronic prodrug of 4-hydroxytamoxifen is more efficacious than tamoxifen with enhanced bioavailability independent of CYP2D6 status. *BMC Cancer*. 2015; 15(1): 1-9.
43. Maximov PY, Abderrahman B, Fanning SW, Sengupta S, Fan P, Curpan RF, *et al.* Endoxifen, 4-hydroxytamoxifen and an estrogenic derivative modulate estrogen receptor complex mediated apoptosis in breast cancer. *Mol Pharmacol*. 2018; 94(2): 812-822.
44. Molina L, Bustamante F, Orloff A, Ramos I, Ehrenfeld P, Figueroa CD. Continuous exposure of breast cancer cells to tamoxifen upregulates GPER-1 and increases cell proliferation. *Front Endocrinol*. 2020; 11.
45. Fröhlich T, Mai C, Bogautdinov RP, Morozkina SN, Shavva AG, Friedrich O, *et al.* Synthesis of tamoxifen-artemisinin and estrogen-artemisinin hybrids highly potent against breast and prostate cancer. *ChemMedChem*. 2020; 15(15): 1473.
46. Kelly PM, Keely NO, Bright SA, Yassin B, Ana G, Fayne D, *et al.* Novel selective estrogen receptor ligand conjugates incorporating endoxifen-combretastatin and cyclofenil-combretastatin hybrid scaffolds: Synthesis and biochemical evaluation. *Molecules*. 2017; 22(9): 1440.
47. Luo G, Li X, Zhang G, Wu C, Tang Z, Liu L, *et al.* Novel SERMs based on 3-aryl-4-aryloxy-2H-chromen-2-one skeleton-a possible way to dual ER α /VEGFR-2 ligands for treatment of breast cancer. *Eur J Med Chem*. 2017; 140: 252-273.
48. Shtaiwi A, Adnan R, Khairuddean M, Khan SU. Computational investigations of the binding mechanism of novel benzophenone imine inhibitors for the treatment of breast cancer. *RSC Advances*. 2019; 9(61): 35401-35416.
49. Wilcken R, Zimmermann MO, Lange A, Joerger AC, Boeckler FM. Principles and applications of halogen bonding in medicinal chemistry and chemical biology. *J Med Chem*. 2013; 56(4): 1363-1388.
50. Liew SK, Malagobadan S, Arshad NM, Nagoor NH. A review of the Structure-Activity Relationship of natural and synthetic antimetastatic compounds. *Biomolecules*. 2020; 10(1): 138.